electronic reprint

JOURNAL OF SYNCHROTRON RADIATION

ISSN: 1600-5775
journals.iucr.org/s

High-efficiency X-ray multilayer-coated blazed gratings with shifted boundaries

Maxim Lubov and Leonid Goray

J. Synchrotron Rad. (2019). **26**, 1539–1545

JOURNAL OF SYNCHROTRON RADIATION

ISSN 1600-5775

Received 5 November 2018
Accepted 4 May 2019

Edited by Y. Amemiya, University of Tokyo, Japan

Keywords: multilayer-coated diffraction grating; soft X-ray range; grating efficiency; growth modeling; multilayer-coated blazed X-ray grating; thin-film growth simulations; diffraction efficiency; electromagnetic diffraction theory.

High-efficiency X-ray multilayer-coated blazed gratings with shifted boundaries

Maxim Lubov[a]* and Leonid Goray[a,b,c]*

[a]St Petersburg Academic University, Khlopin St 8/3 Let A, St Petersburg 194021, Russian Federation, [b]ITMO University, Kronverkskiy prospekt 49, St Petersburg 197101, Russian Federation, and [c]Institute for Analytical Instrumentation, Rizhsky prospekt 26, St Petersburg 190103, Russian Federation. *Correspondence e-mail: lubov@spbau.ru, lig@pcgrate.com

A new design for a high-efficiency multilayer-coated blazed X-ray grating with horizontal-shifted (non-conformal) boundary profiles is proposed. The investigation of the grating design is carried out using an integrated approach based on rigorous numerical calculations of light diffraction by gratings with realistic boundary profiles obtained from simulations of multilayer grating growth. By varying the incidence angle of the deposition flux, one can set the direction and magnitude of the boundary profile shifts over a wide range of values. It is shown that the diffraction efficiency of the blazed gratings with shifted boundary profiles may be substantially higher than the efficiency of gratings with conformal boundaries, which are, moreover, much more difficult to produce. High-efficiency gratings with shifted boundaries can be obtained when the deposition is mainly on the blaze facet with a high inclination of the deposition flux, as opposed to widely used near-normal deposition methods. The maximum absolute efficiency of a W/B4C 2500 mm^{-1} grating with a blaze angle of 1.76° and an anti-blaze angle of 20°, working at a blaze wavelength of 1.3 nm and having shifted realistic boundary profiles, obtained using our integrated approach is 23.3%, while that of a grating with the ideal (triangular) boundary profile and the same shifts is 25.3%, and that of an ideal conformal profile is only 22.2%. The maximum absolute efficiency of 40.2% of a 2500 mm Cr/C grating with a blaze angle of 1.05° and a realistic anti-blaze angle of 10°, working at a blaze wavelength of 0.83 nm and having ideal shifted boundaries, is higher than the maximum efficiency of the similar grating having ideal conformal boundaries with a non-realistic anti-blaze angle of 80°.

1. Introduction

Multilayer-coated blazed gratings (MBGs) are considered the most promising optical structures for many hard and soft X-ray applications (Rife *et al.*, 1990; Spiller, 1994). One of the main requirements to be met by MBGs is the high diffraction efficiency η. This requirement can be achieved through improvements in the grating design and in the controlled fabrication of a multilayer structure, accounting for peculiarities of the growth process, such as smoothing of boundary profiles, interlayer mixing and surface roughness development. Recently, a number of studies have been conducted in which different ways to improve the efficiency of soft X-ray MBGs have been considered (Voronov *et al.*, 2015; Goray & Egorov, 2016; Senf *et al.*, 2016). It was shown by Voronov *et al.*, (2015, 2016) that gratings with high groove densities allow high grating efficiencies to be achieved at a very high resolution in the soft X-ray and extreme ultraviolet range. It was demonstrated (Senf *et al.*, 2016) that a saw-tooth profile has to be ruled into a gold-coated surface and then reactive ion etching transfers the profile onto the substrate. Another way

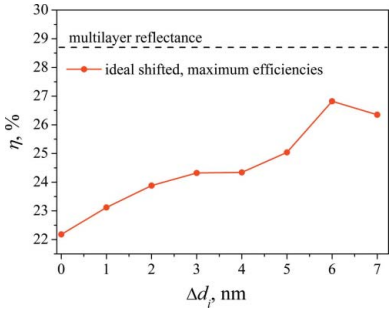

to increase grating efficiency in the soft X-ray range is to implement another diffraction scheme, *i.e.* a conical one (Goray & Egorov, 2016). Compared with classical schemes (in-plane diffraction), conical diffraction reduces negative effects, *e.g.* absorption and refraction, and eventually leads to a higher efficiency. However, deformation of MBG boundary profiles and their shifts during growth significantly decrease efficiency (Voronov *et al.*, 2011*a*). The geometric shape of the profiles changes during growth, owing to smoothing, deposition source noise and various nonlocal effects such as shadowing and re-emission (Pellicione & Lu, 2007). Deformation of the boundary profiles in the case of strong smoothing can transform the saw-tooth profile into a sinusoidal one (Voronov *et al.*, 2011*b*). Deposition noise not only affects the root-mean-square surface roughness but also leads to the evolution of the initial surface topography into a complex structure characterized by a set of roughnesses and correlation lengths (Senthilkumar *et al.*, 2005; Yashchuk *et al.*, 2014; Goray & Lubov, 2015). Nonlocal effects can significantly transform the grating boundaries, since a local growth event occurring at some point on the profile surface influences the growth process at a great distance from the original event.

Thus, an investigation of the design of MBGs should include both an accurate calculation of diffraction characteristics, taking into account realistic boundary profiles, and a simulation of the evolution of the initial profile during growth. The most effective approach to calculating diffraction grating efficiencies would be to use rigorous numerical methods, since they, unlike analytical and approximate calculations, allow one to take complex boundary profiles, random roughness and changes in the composition of layers exactly into account (Goray & Schmidt, 2014). Boundary profiles can either be obtained from a numerical calculation of the growth process or derived from transmission electron microscopy (TEM) measurements. However, TEM determination of boundary profiles is destructive and ineffective, since such measurements are necessary for each growth experiment and for many periods and grating boundaries, the number of which can reach hundreds. It is also necessary not only to determine boundary profiles and their random roughnesses but also the composition of layers, since this affects complex-valued refractive indices (Gullikson, 2019). Therefore, a theoretical approach based on the modeling of layer growth, with subsequent computations of the scattering intensity of a simulated structure, is more effective in the design of multilayer gratings working in the shortest wavelength range.

For the first time, to the best of our knowledge, this integrated approach was proposed by Goray & Lubov (2013) to calculate the absolute efficiencies of multilayer Mo/Si and Al/Zr gratings, working in the extreme ultraviolet range. This approach was also successfully applied to the consideration of the growth of rough multilayer mirrors and the calculation of scattering intensities in the soft X-ray and extreme ultraviolet ranges (Goray & Lubov, 2015). The use of this approach allowed the shift and deformation of the profile during the growth of Al/Zr gratings to be explained (Voronov *et al.*, 2011*a*,*b*). It was shown that deposition of the material on the asymmetrical profile leads to a horizontal shift in the boundary profiles. However, the dependence of the profile shift on the incidence angle of the deposition flux remains unknown. Calculation of this dependence allows one to choose the optimal incidence angle and estimate how the initial profile changes during growth. Moreover, the question arises of how the diffraction efficiency depends on the shifts of the boundary profiles. According to the prediction of scalar diffraction theory, for blazed gratings with angle ζ at the top of a profile equal to 90°, 100% efficiency is achieved with a conformal [see Fig. 1(*a*)] arrangement of the layers at one polarization (Voronov *et al.*, 2015; Nevière & Montiel, 1996). However, for state-of-the-art short-period soft X-ray gratings with $\zeta > 90°$ and β (the anti-blaze angle) equal to several degrees or several tens of degrees, the configuration of the layers corresponding to maximum efficiency is unknown. Therefore, to determine the configuration of the grating layers that corresponds to the maximum efficiency, it is necessary to calculate and compare diffraction efficiencies of gratings with conformal and non-conformal [see Fig. 1(*b*)] boundary profiles.

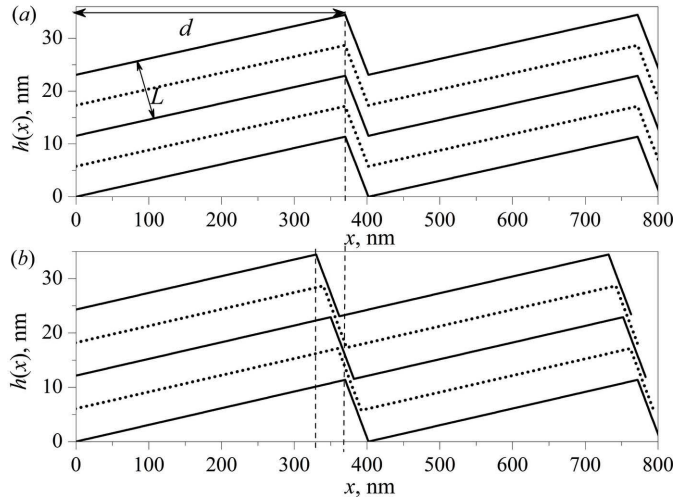

Figure 1
Schematic view of (*a*) conformal and (*b*) non-conformal multilayer-coated grating geometries. The period of the grating is d and the period of the multilayer coating is L.

In this manuscript, on the basis of the simulations of the growth of W/B_4C and Cr/C MBGs and rigorous calculations of their diffraction efficiencies, we demonstrate that MBGs with shifted boundary profiles may have higher diffraction efficiencies than similar MBGs with conformal layers.

2. Growth simulation

The growth process is considered within the continuous approach (Pellicione & Lu, 2007; Villain, 1991). This approach allows us to model MBGs growth over large scales, both spatially, with the grating period $d \simeq 10^1$–10^4 nm, and temporally, with a growth time of the order of 10^2–10^3 s. This approach has proven effective in the study of growth on patterned-surface substrates (Goray & Lubov, 2013;

De Virgilis *et al.*, 2003; Ballestad *et al.*, 2005; Castez, 2010; Harrison & Bradley, 2017).

The grating profile can be considered isotropic and two-dimensional; therefore, we represent the profile height h as a function of coordinate x and time t. The evolution of the boundary profile is calculated with the help of the Mullins equation (Mullins, 1957), in which the local surface curvature $K(x, t)$ is strictly taken into account:

$$\frac{\partial h(x,t)}{\partial t} = g(x,t) - \nu_4 \frac{\partial}{\partial x}\left(\left\{1 + \left[\nabla h(x,t)\right]^2\right\}^{-1/2} \frac{\partial K}{\partial x}\right). \quad (1)$$

Here $g(x, t)$ is the density of the deposition flux and ν_4 is the smoothing coefficient, determined by the surface diffusion coefficient and surface free energy (Mullins, 1957). The explicit expression for $K(x, t)$ can be found in Polyanin & Manzhirov (2006). The flux of atoms on the surface of a grating with a triangular profile is defined by the blaze angle φ, β, and the deposition flux incidence angle α measured from the horizon counterclockwise, where $\alpha = 0$ corresponds to the horizontal flux striking only the anti-blaze facet. In these calculations, we do not consider shadowing effects; therefore, φ, β and α should be related by $\varphi < \alpha$ and $\beta < 180 - \alpha$. The deposition flux to the blaze facet can be written (taking into account the condition of non-shadowing) as (Goray & Lubov, 2013)

$$g(x,t) = I_0 \sin[\alpha - \varphi(x,t)]. \quad (2)$$

Here, I_0 is the value of the deposition flux emitted from the source and $\varphi(x, t) = \arctan[\nabla h(x, t)]$. Similarly, for the flux deposited on the anti-blaze facet, we have

$$g(x,t) = I_0 \sin[\alpha + \beta(x,t)]. \quad (3)$$

Here, $\beta(x, t) = \arctan[|\nabla h(x, t)|]$. Other mechanisms of layer growth are not considered in this work, for example, when growth occurs along the local surface normal [Kardar–Parisi–Zhang equation (Kardar *et al.*, 1986)] or when diffusion between the layers with a sharp change in composition is significant [Cahn–Hilliard equation (Cahn & Hilliard, 1958)]. This is because the purpose of our research is to investigate how a change in the incidence angle of the deposition flux affects the shift of boundaries. The shift, as shown by Goray & Lubov (2013), is caused by a non-uniform distribution of the material on the profile surface, which is, in turn, determined by α. In the case of other growth mechanisms, the boundary profile shift still occurs and only the shift values change.

The smoothing coefficients (ν_4) in the growth simulation were chosen on the basis that in order to obtain high diffraction efficiencies it is necessary to ensure that smoothing is sufficiently small in such a growth mode Significant smoothing of the grating boundary profile means that a non-optimal growth mode is realized (Goray & Lubov, 2013).

3. Results and discussion

3.1. W/B_4C grating

The grating growth was calculated for a W/B_4C MBG with the following parameters (Voronov *et al.*, 2016): $\varphi = 1.76°$, $\beta = 20°$, $d = 402$ nm (d is the grating period), $\Gamma = 0.5$ (Γ is the ratio of the thickness of a layer to the period of the multilayer coating), $L = 5.78$ nm (L is the period of the multilayer coating) and $n = 18$ (n is the number of bilayers). The shift of the boundary profiles $\Delta d_i(\alpha)$ for the ith layer boundary ($i = 1, 2, \ldots, n$) can be calculated using $\Delta d_i(\alpha) = x(h_s) - x(h_i)$. Here, h_s and h_i are the x coordinates of the maximum profile height of the substrate and ith layer boundary, respectively.

Fig. 2 shows the dependences of Δd on α and i. Calculations were carried out with $I_0 = 1$ nm s^{-1}, with $\nu_4 = 25$ nm^4 s^{-1} in the first layer and $\nu_4 = 20$ nm^4 s^{-1} in the second layer. As can be seen from Fig. 2(*a*), the dependence of Δd_1 on α is almost linear in the range $\alpha = 60$–$140°$ and increases rapidly for $\alpha > 140°$, whereas the dependence of Δd on i (with $\alpha = 150°$) is linear for all i, as shown in Fig. 2(*b*). The shift in the profile is caused by the non-uniform deposition of the material (Goray & Lubov, 2013), and therefore the increase in profile height is also non-uniform. The non-uniformity leads to redistribution

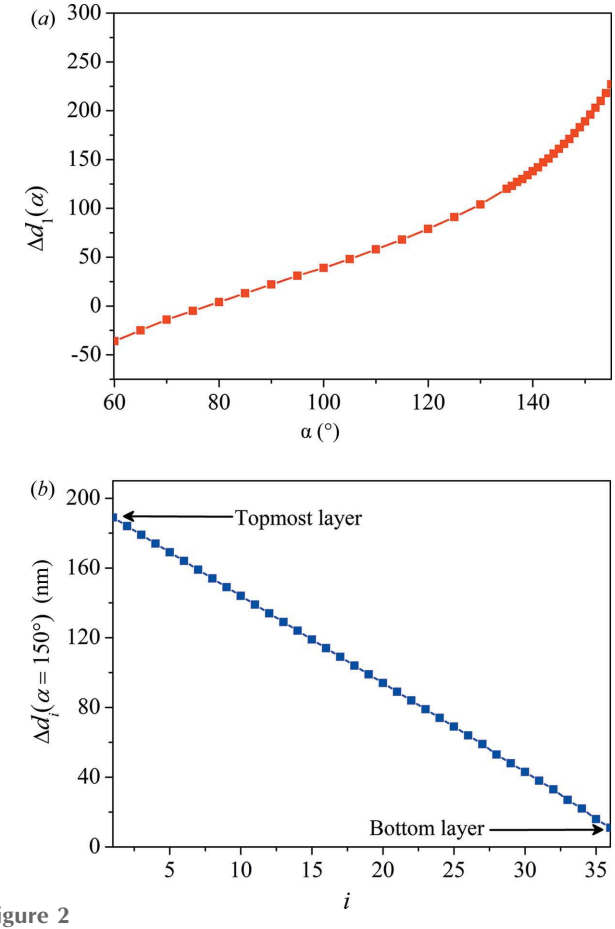

Figure 2
Dependences calculated for a W/B_4C grating with $\varphi = 1.76°$ and $\beta = 20°$: (*a*) shift of the grating topmost boundary profile versus the deposition flux incidence angle; (*b*) shift of the grating boundary profile ($\alpha = 150°$) versus the number of layers.

of the material and smoothing of the profile. The magnitude of the shift depends on the ratio of the fluxes to different facets of the profile. Since the fluxes to the facets are determined by φ, β and α, equality of the fluxes is achieved when $f(x) = \sin[\alpha - \varphi(x,t)]/\sin[\alpha + \beta(x,t)] = 1$. The behavior of $f(x)$ is linear when α = 60–120° for the considered profile angles and increases rapidly for larger α. However, the transition of $f(x)$ from linear to nonlinear behavior depends on β. The smaller the value of β, the greater the value of α at which the transition to nonlinear behavior occurs. During smoothing of the profile, β becomes smaller and therefore the transition from linear behavior to nonlinear occurs at larger β.

The linear dependence of Δd on i is mostly caused by the establishment of a steady-state smoothing mode, at which deposition fluxes on the facets near the maximum profile height become approximately equal some time after the beginning of deposition.

The change in α affects not only the position of the boundaries of the layer but also the profile height. The change in profile height $\Delta h_i(\alpha)$ for the ith layer boundary can be calculated using $\Delta h_i(\alpha) = h_s - h_i$. Fig. 3 shows the dependences of h_i and Δh_i on α and i. The inset figure shows parts of the initial profile and topmost profiles at α = 60° and 150°,

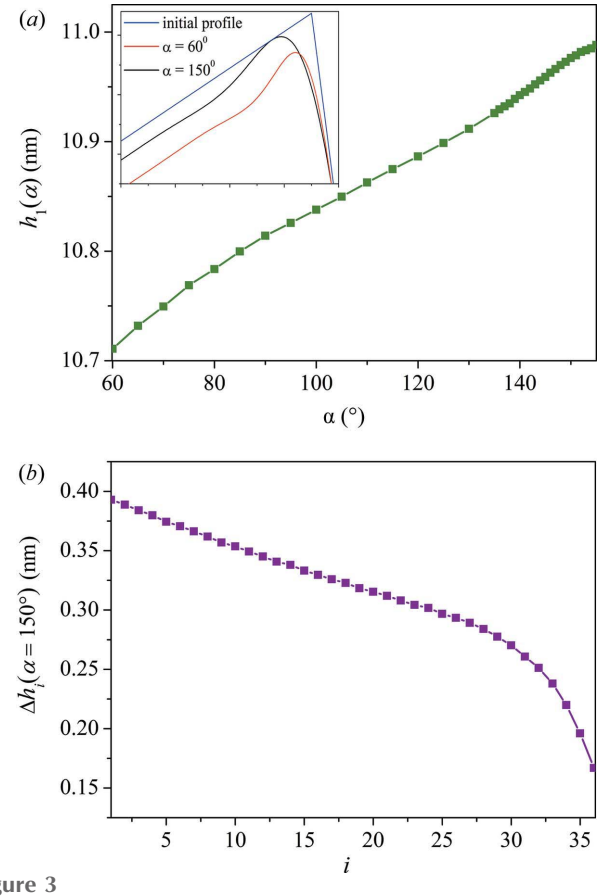

Figure 3
Dependences calculated for a W/B_4C grating with φ = 1.76° and β = 20°: (*a*) height of the grating topmost boundary profile versus the deposition flux incidence angle; (*b*) height change of grating (α = 150°) versus the number of layers. Inset: view of the upper parts of the topmost boundary profiles obtained for different deposition flux incidence angles.

Table 1
Maximum diffraction efficiency η for the W/B_4C grating with φ = 1.76° and β = 20°, calculated for various boundary shifts.

Boundaries	α (°)	θ (°)†	Δd_1 (nm)	Δh_1 (nm)	η (%)
Ideal shifted	60	84.4	−25	0	21.7
	150	84.9	189	0	25.3
Ideal conformal		84.5	0	0	22.2
Realistic shifted	60	84	−25	0.65	10.2
	70	83.9	−14	0.62	17.4
	135	84.5	120	0.43	22.6
	150	84.5	189	0.39	23.3

† θ is the radiation incidence angle at which maximum efficiency is achieved.

shifted for convenience of comparison. As one can see from Fig. 3, the greater the value of α, the smaller the value of $h_1(\alpha)$ during growth.

It is worth noting that calculations made for different values of ν_4 have shown that an increase in ν_4 leads to: (i) an additional shift of the boundaries to the left (along the blaze facet) and (ii) stronger profile smoothing and a greater decrease in profile height.

The diffraction efficiencies of gratings with realistic and ideal boundary profiles were calculated using the rigorous boundary integral equation method (Goray & Schmidt, 2014). This method has been successfully used in the modeling of efficiencies and scattering intensities of different multilayer structures used in the soft X-ray and extreme ultraviolet regions, *e.g.* gratings, rough mirrors or zone plates (Goray & Schmidt, 2014; Seely *et al.*, 1999; Goray *et al.*, 2006; Goray, 2010). The diffraction efficiencies of the MBGs were calculated using the commercial program *PCGrate-SX* (version 6.7; http://pcgrate.com).

The results of the calculations demonstrate that the shift of the grating boundaries has a significant effect on η. A shift of the profile to the right, $\Delta d < 0$, leads to a reduction in efficiency, while a shift to the left, $\Delta d > 0$, leads to an increase in efficiency; see Table 1. For gratings with ideal shifted boundaries, values of $\Delta d_i(\alpha)$ were taken from simulation results corresponding to realistic shifted boundaries. The results presented in Table 1 show that the grating efficiencies with both realistic η_r and ideal η_{id} boundaries change in the same way. Moreover, the efficiency of the gratings with ideal conformal boundaries is smaller than the efficiency of gratings with shifted realistic boundaries for α = 150°. Such efficiency behavior is unexpected and suggests opportunities for the fabrication of new, more efficient and easy-to-produce MBGs.

For a more detailed understanding of the efficiency behavior, high-accuracy computations for MBGs with realistically grown profiles were made at α = 135–150°. Fig. 4 presents the efficiencies of the gratings with conformal and non-conformal boundaries. As can be seen from Fig. 4, the efficiency generally increases with increasing deposition angle; however, $\eta(\alpha)$ may have local minima and maxima. The ratio between η_{id} and η_r is greater for small α. Hence, it can be concluded that the rapid decrease in efficiency is mostly caused by the decrease in

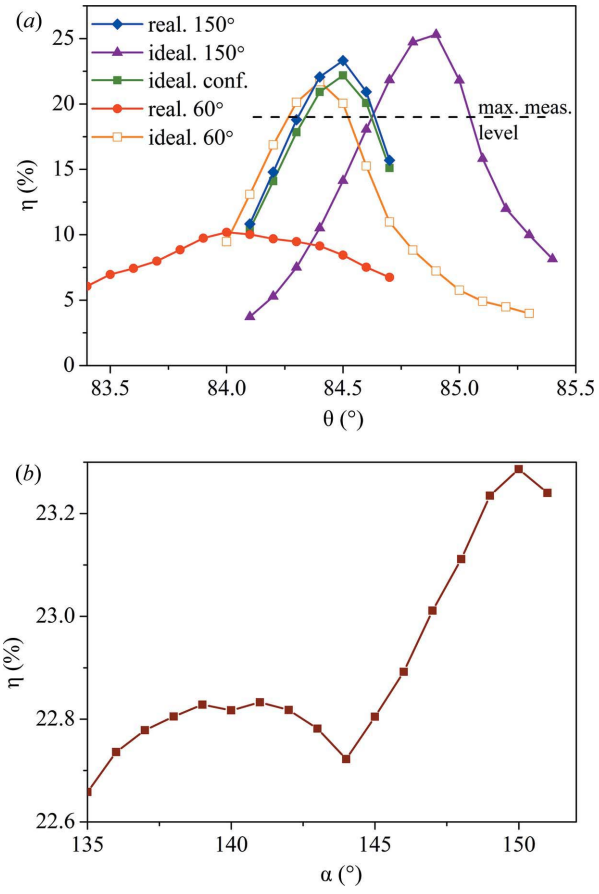

Figure 4
Dependences calculated for the W/B_4C grating with $\varphi = 1.76°$ and $\beta = 20°$: (*a*) efficiency versus radiation incidence angle for realistic and ideal boundary profiles; (*b*) efficiency versus flux incidence angle for shifted realistic boundary profiles.

profile height. The difference in realistic profile heights $h(x, t)$ of the topmost boundaries for $\alpha = 60°$ and 150° is only 0.26 nm or 2% of the initial height, and the value of the efficiency is more than halved (56%), whereas for the gratings with ideal shifted boundaries, $\Delta h = 0$, the efficiency decreases by only 14%. We suppose that such dependences are caused by the complex interplay between boundary shifts and changes in profile height during growth. Indeed, the efficiency of an MBG depends on various processes occurring during diffraction, *i.e.* absorption, multiple reflection and refraction, shadowing, *etc*. Meanwhile a contribution of all these processes to the efficiency is affected by the structure of the layers, *i.e.* the boundary shifts and depths of the layers on the blaze and anti-blaze facets. Therefore, although the growth of MBGs with the layer structure leads to an increase in efficiency with increasing α, a specific set of structural parameters might not be optimal.

In Fig. 5, results of calculations of the diffraction efficiency of the W/B_4C grating with ideal shifted boundaries and the constant shift Δd_i for all boundaries versus shift of the boundary profile are shown. As one can see, the behavior is non-linear and there is an optimal shift value which corresponds to the maximal efficiency and minimal absorption.

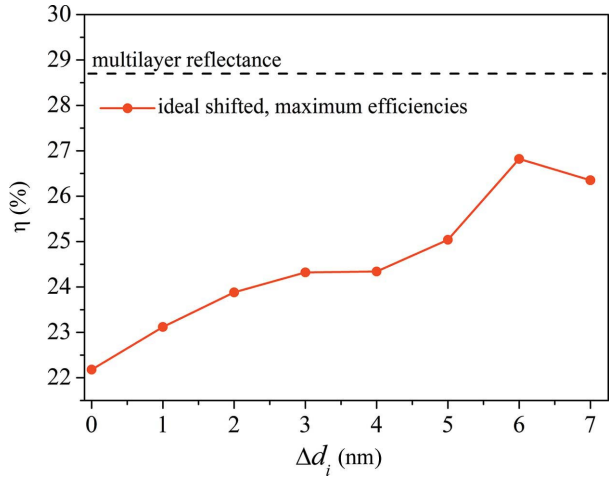

Figure 5
Maximal efficiency of the W/B_4C grating with $\varphi = 1.76°$ and $\beta = 20°$, and ideal boundaries versus shift of the boundary profile.

3.2. Cr/C grating

In connection with the results obtained for W/B_4C MBGs, the question arises whether a similar change in the efficiency is observed for other sawtooth gratings with non-conformal geometries. In order to study the influence of the shift of the boundary profiles, calculations of growth and diffraction efficiencies were performed for the Cr/C MBG. Parameters of the grating included $\varphi = 1.05°$, $d = 400$ nm and $\beta = 10°$; multilayer Cr/C parameters were taken from the literature (Senf *et al.*, 2016): $\Gamma = 0.6$, $L = 7.3$ nm and $n = 20$. This grating has a flatter profile and can work at an optimal wavelength of 0.83 nm (1.5 keV) in the −1st order. Calculations of the grating growth were carried out with $I_0 = 1$ nm s^{-1}, with $\nu_4 = 25$ nm^4 s^{-1} in the first layer and $\nu_4 = 20$ nm^4 s^{-1} in the second layer, which is the same for W/B_4C gratings.

A flatter initial profile in the case of Cr/C MBG leads to less smoothing of the profile during growth, and hence to a lesser effect of the deformation of the profile on the efficiency. Indeed, for $\alpha = 150°$ the reduction in height Δh for the Cr/C MBG is about 0.3 nm for $L = 7.3$ nm and $n = 20$, whereas, for the W/B_4C MBG with $L = 5.78$ nm and $n = 18$, the value of Δh is equal to 0.39 nm (see Table 1).

It should be noted that the profile deformation during growth, *i.e.* the boundary profile shift and the change in its height are determined by the geometry of the profile and the relaxation mechanism, which were the same in both MBG cases. In this regard, the dependencies of changes in the profile height and shifts on α and i are similar for W/B_4C and Cr/C MBGs and therefore the results of growth calculations are presented here only for the W/B_4C MBGs.

For Cr/C gratings with ideal shifted boundaries, Δd_i values were held constant for all layers of the considered MBG. The results of the Cr/C efficiency calculations, as in the case of W/B_4C gratings, demonstrate that the shift of the grating boundaries to the left, $\Delta d > 0$, leads to an increase in efficiency (Fig. 6). In opposition to the shifts to the left, even a small shift to the right leads to a significant decrease in efficiency.

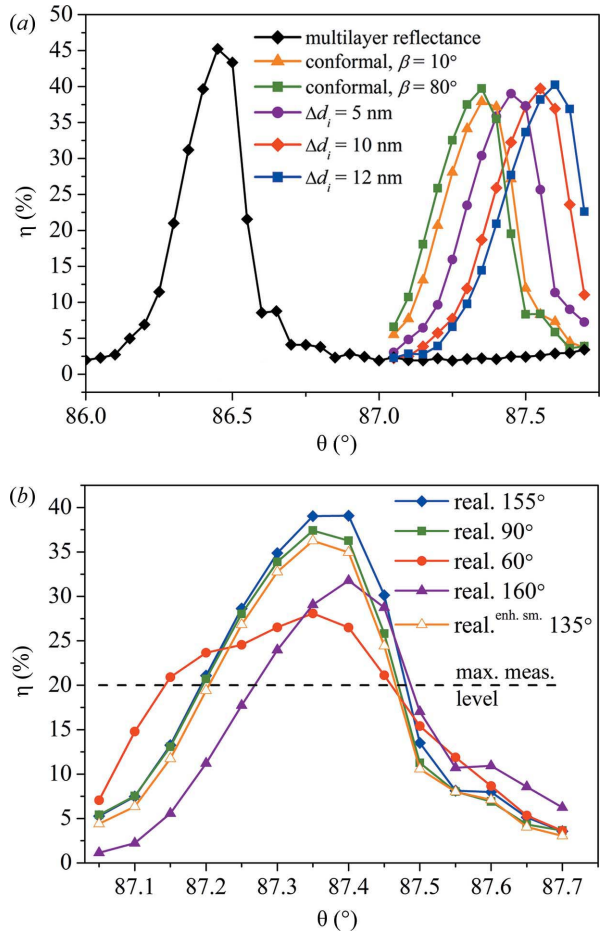

Figure 6
Efficiencies calculated for the Cr/C grating with $\varphi = 1.05°$, and $\beta = 10°$ or $\beta = 80°$ versus radiation incidence angle: (*a*) for ideal conformal and ideal shifted boundary profiles; (*b*) for realistic shifted boundary profiles (enh.sm. corresponds to enhanced smoothing of the grating calculated for $\nu_4 = 250\ \mathrm{nm^4\ s^{-1}}$ in the first layer and $\nu_4 = 200\ \mathrm{nm^4\ s^{-1}}$ in the second layer).

As shown in Fig. 6, the maximal absolute efficiency (40.2%) of the MBG with a realistic anti-blaze angle of 10° and ideal shifted boundaries is higher than the maximal efficiency (39.7%) of similar grating having ideal conformal boundaries with a non-realistic anti-blaze angle of 80°. Moreover, these efficiencies are only slightly higher than the maximal efficiency of 39.2% of the MBG with realistic shifted boundaries [Fig. 6(*b*)]. The maximal efficiency of the Cr/C MBG with realistic boundaries is reached at $\alpha = 155°$, while at $\alpha = 160°$, the diffraction efficiency decreases significantly and the absorption increases. We also considered the case of shifting upper boundary profiles to the left by more than the period of grating $d = 400$ nm. For example, at the angle $\alpha = 160°$ for the fourth layer from the top, the value of the shift from the initial (substrate) profile position is equal to 408 nm, and the topmost layer is shifted by 435 nm. In the case of such a strong shift, upper layers of the grating, which impact efficiency the most, could be considered as shifted to the right relative to the initial (substrate) profile position.

4. Conclusions

Thus, we found that MBGs with conformal boundaries do not have the highest efficiency in the soft X-ray range; on the contrary, MBGs with appropriately horizontal-shifted boundary profiles are more efficient, taking into account realistic anti-blaze angle values and the decreasing absorption. Moreover, the efficiency of gratings with realistic boundary profiles has a complex dependence on profile shifts and height reductions. Therefore, any search for optimal MBGs should be based on exact calculations or measurements of the grating boundary cross-section and efficiency.

We have demonstrated that the diffraction efficiency of the MBGs with shifted boundary profiles may be substantially higher than the efficiency of gratings with conformal boundaries, which are, moreover, much more difficult to produce. Based on our results, a new design of the soft X-ray MBGs could be proposed. The principal new idea of the proposed design is to fabricate MBGs with the layers highly shifted toward the direction of the incidence radiation, *i.e.* along the anti-blaze facet of the profile. The strong shift of the boundary profiles in the desired direction is achieved when deposition occurs predominantly on the blaze facet. In the manufacture of such gratings, it is necessary to set the incidence angle of the deposition flux in the range at which most of particles are deposited on the blaze facet, while the anti-blaze facet is not shaded from the deposition flux.

Funding information

This work was partially supported by the Ministry of Education and Science of the Russian Federation, the Russian Foundation for Basic Research (RFBR) (grant No. 16-29-11697) and Russian Science Foundation (RSF) (grant No. 19-12-00270).

References

Ballestad, A., Lau, B., Schmid, J. H. & Tiedje, T. (2005). *Mater. Res. Soc. Symp. Proc.* 859E, JJ9.6.1.
Cahn, J. W. & Hilliard, J. E. (1958). *J. Chem. Phys.* **28**, 258–267.
Castez, M. F. (2010). *J. Phys. Condens. Matter*, **22**, 345007.
De Virgiliis, A., Azzaroni, O., Salvarezza, R. C. & Albano, E. V. (2003). *Appl. Phys. Lett.* **82**, 1953–1955.
Goray, L. I. (2010). *J. Appl. Phys.* **108**, 033516.
Goray, L. I. & Egorov, A. Yu. (2016). *Appl. Phys. Lett.* **109**, 103502.
Goray, L. & Lubov, M. (2013). *J. Appl. Cryst.* **46**, 926–932.
Goray, L. I. & Lubov, M. N. (2015). *Opt. Express*, **23**, 10703–10713.
Goray, L. I. & Schmidt, G. (2014). *Gratings: Theory and Numerical Applications*, edited by E. Popov, ch. 12. Marseille: Presses Universitaires de Provence.
Goray, L. I., Seely, J. F. & Sadov, S. Yu. (2006). *J. Appl. Phys.* **100**, 094901.
Gullikson, E. M. (2019). *X-ray Database*, http://henke.lbl.gov.
Harrison, M. P. & Bradley, R. M. (2017). *J. Appl. Phys.* **121**, 054308.
Kardar, M., Parisi, G. & Zhang, Y. (1986). *Phys. Rev. Lett.* **56**, 889–892.
Mullins, W. W. (1957). *J. Appl. Phys.* **28**, 333–339.
Nevière, M. & Montiel, F. (1996). *J. Opt. Soc. Am. A*, **13**, 811–818.
Pellicione, M. & Lu, T. M. (2007). *Evolution of Thin Film Morphology – Modelling and Simulations.* Berlin: Springer.

Polyanin, A. D. & Manzhirov, A. V. (2006). *Handbook of Mathematics for Engineers and Scientists.* Boca Raton: Chapman and Hall/CRC.
Rife, J. C., Barbee, T. W. Jr, Hunter, W. R. & Cruddace, R. G. (1990). *Phys. Scr.* **41**, 418–421.
Seely, J. F., Goray, L. I., Hunter, W. R. & Rife, J. C. (1999). *Appl. Opt.* **38**, 1251–1258.
Senf, F., Bijkerk, F., Eggenstein, F., Gwalt, G., Huang, Q., Kruijs, R., Kutz, O., Lemke, S., Louis, E., Mertin, M., Packe, I., Rudolph, I., Schaefers, F., Sokolov, F., Sturm, M., Waberski, Ch., Wang, Z., Wolf, J., Zeschke, T. & Erko, A. (2016). *Opt. Express*, **24**, 13220–13230.
Senthilkumar, M., Sahoo, N. K., Thakur, S. & Tokas, R. B. (2005). *Appl. Surf. Sci.* **252**, 1608–1619.
Spiller, E. (1994). *Soft X-ray Optics*. Belingham, Washington: SPIE.
Villain, J. (1991). *J. Phys. I*, **1**, 19–42.
Voronov, D. L., Anderson, E. H., Cambie, R., Cabrini, S., Dhuey, S. D., Goray, L. I., Gullikson, E. M., Salmassi, F., Warwick, T., Yashchuk, V. V. & Padmore, H. A. (2011*a*). *Opt. Express*, **19**, 6320–6325.
Voronov, D. L., Anderson, E. H., Cambie, R., Gullikson, E. M., Salmassi, F., Warwick, T., Yashchuk, V. V. & Padmore, H. A. (2011*b*). *Proc. SPIE*, **8139**, 81390B.
Voronov, D. L., Goray, L. I., Warwick, T., Yashchuk, V. V. & Padmore, H. A. (2015). *Opt. Express*, **23**, 4771–4790.
Voronov, D. L., Salmassi, F., Meyer-Ilse, J., Gullikson, E. M., Warwick, T. & Padmore, H. A. (2016). *Opt. Express*, **24**, 11334–11344.
Yashchuk, V. V., Tyurin, Y. N. & Tyurina, A. Yu. (2014). *Opt. Eng.* **53**, 084102.